INTERNATIONAL JOURNAL FOR NUMERICAL METHODS IN FLUIDS, VOL. 9, 531–540 (1989)

MATHEMATICAL DERIVATION OF A FINITE VOLUME FORMULATION FOR LAMINAR FLOW IN COMPLEX GEOMETRIES

LARS DAVIDSON AND PETER HEDBERG

Department of Applied Thermodynamics and Fluid Mechanics, Chalmers University of Technology, S-412 96 Gothenburg, Sweden

SUMMARY

This paper treats the mathematical derivation of a novel formulation of the Navier–Stokes equation for general non-orthogonal curvilinear co-ordinates. The covariant velocity components are solved in this FVM formulation, which leads to the pressure–velocity coupling becoming relatively easy to handle at the expense of a more complicated expression of the convective and diffusive fluxes. When a velocity component is solved at a point P, the neighbouring velocities are projected in the direction of the velocity component at the point P. Thus the base vectors are changed at the neighbouring points. This renders a simpler expression for the covariant derivatives. Neither the Cristoffel symbol nor its derivatives need be computed. This contributes to the accuracy of the formulation. The procedure of changing the base vectors affects only the convected velocity. The convecting term (dot product of velocity and area) is calculated without any change of the base vectors. The same is true for the operator on the covariant velocity in the diffusion term.

It is shown that when using upwind differencing the use of projected velocities gives better results than when curvature effects are included in the source term. The discretized equations are written in a form which enables the use of the tridiagonal matrix algorithm (TDMA). The equations can be solved using either the SIMPLEC or the PISO procedure.

Two examples of laminar flows are given.

KEY WORDS General non-orthogonal Complex geometries Viscous

1. INTRODUCTION

Many applications, such as vehicle dynamics, turbomachinery and aerodynamics, have complex geometric configurations. It is essential when simulating flow for these types of configurations that boundary-fitted co-ordinates (where the co-ordinate lines follow the boundaries) are used.

Much work has been done in developing and applying finite volume methods to complex geometries. In some of the work, general orthogonal co-ordinates have been used.[1–3] The advantage of using orthogonal co-ordinates rather than non-orthogonal co-ordinates is that the equations become much simpler; the disadvantage is the reduced flexibility when generating the grid.

Other researchers have used non-orthogonal co-ordinate systems. A choice has to be made when representing the velocity vector and some have chosen covariant velocity components,[4–6] others contravariant[7–9] and still others physical velocity components.[10] Using covariant velocity components means that the pressure–velocity coupling becomes relatively easy to handle at the expense of the more complicated expression of convective and diffusive fluxes. For contravariant

0271–2091/89/050531–10$05.00

Received 11 December 1987
Revised 26 July 1988

and physical velocity components the problems are reversed. Covariant velocity components have been chosen in this work.

The approach taken here is to set up a local rectilinear co-ordinate system where the co-ordinate axis, in the direction of the $(v_1)_P$-velocity component, is kept constant in the neighbourhood of point P. This means that most of the terms due to the curvature/divergence and non-orthogonality of the grid vanish. The procedure of keeping the co-ordinate axis constant (i.e. $\mathbf{g}_i = \text{constant}$) in the immediate vicinity of point P affects the convected velocity only. The convecting velocity (convection, i.e. dot product of the velocity vector and the area vector) is calculated without any change of the base vectors. This is also the case for the diffusion term.

This approach has been previously adopted by Karki[5] and partly by Malin *et al.*[4] In neither of these works was the mathematical derivation shown.

The code here is applied to two laminar test cases: uniform flow across a polar grid and the flow in an expanding channel.

2. DERIVATION OF THE DISCRETIZED EQUATIONS

The steady incompressible momentum equation can be written in general co-ordinates, using covariant components, as[11]

$$v^k v_{i,k} = -\frac{1}{\rho}\frac{\partial P}{\partial x^i} + \nu g^{jk} v_{i,jk}, \tag{1}$$

where g^{jk} denotes the contravariant components of the metric tensor. The convention that subscripts (i, j, k) denote covariant components and superscripts (i, j, k) denote contravariant components is used throughout the paper. Covariant components are chosen because this gives the simplest expression of the pressure gradient, which means that the velocity–pressure coupling becomes relatively easy to handle.

The coma notation (see equation (1)) is used for denoting the covariant derivative, i.e.[12]

$$v_{i,j} \equiv \frac{\partial v_i}{\partial x^j} - \begin{Bmatrix} k \\ i\ j \end{Bmatrix} v_k, \tag{2}$$

where $\{^k_{ij}\}$ denotes the Cristoffel symbol of the second kind. The second term on the RHS of equation (2) is due to the covariant base vectors $\mathbf{g}_i$ not being constant, i.e. the grid lines curve and/or converge/diverge (the $\mathbf{g}_i$ are parallel with the grid lines). This can be shown by rewriting the second term in equation (2) as[13,14]

$$v_k \{^k_{ij}\} = v_k \mathbf{g}^k \cdot \frac{\partial \mathbf{g}_i}{\partial x^j} = \mathbf{v} \cdot \frac{\partial \mathbf{g}_i}{\partial x^j},$$

which, together with equation (2), gives

$$v_{i,j} = \frac{\partial v_i}{\partial x^j} - \mathbf{v} \cdot \frac{\partial \mathbf{g}_i}{\partial x^j}. \tag{3}$$

The LHS of equation (1) can, by using the continuity equation

$$v^k{}_{,k} = 0,$$

be cast in conservative form so that

$$v^k v_{i,k} = v^k v_{i,k} + v_i v^k{}_{,k} = (v^k v_i)_{,k} = (g^{jk} v_j v_i)_{,k}. \tag{4}$$

The k-superscript was lowered by using the relation between covariant and contravariant components[12]

$$v^k = g^{jk} v_j.$$

Multiplication of equation (1) by $\mathbf{g}^i$ and integration of equation (1), using equation (4), over a control volume (the bounded surface of which is denoted by S) gives (see Appendix)

$$\int_S g^{jk}(v_i v_j - \nu v_{i,j}) n_k \mathbf{g}^i \, dS + \frac{1}{\rho} \int_S p n_i \mathbf{g}^i \, dS = 0, \tag{5}$$

where n_k denotes the normal unit vector of the area S. The curvature effects are inherent in equation (5) in two ways: the covariant derivative (see equation (3)) in the diffusion term and the change of the base vectors $\mathbf{g}^i$ over the area S.

If we change the base vectors $(\mathbf{g}_i)_{nb}$ (nb = neighbours) in the immediate surroundings of point P so that they are parallel with $(\mathbf{g}_i)_P$ (see Figure 1 and Appendix), we can replace the covariant derivative $(v_{i,j})$ in equation (5) with the usual derivative $(\partial v_i / \partial x^j)$ (see equation (3)) and we can cancel the base vectors $(\mathbf{g}^i)$. Note that the base vector is constant over a velocity control volume in the second integral (see Figure 1). Equation (5) then gives

$$\int_S g^{jk} \left(v_i v_j - \nu \frac{\partial v_i}{\partial x^j} \right) n_k \, dS + \frac{1}{\rho} \int_S p n_i \, dS = 0. \tag{6}$$

It should be stressed that when the procedure of changing the base vectors is carried out, this affects the v_i-velocity (in equation (5)) *only*, i.e. the convected velocity. The convecting velocity, which appears in the (dot) product

$$g^{jk} v_j n_k = v^k n_k = \mathbf{v} \cdot \mathbf{n}, \tag{7a}$$

is calculated *without* any change of the base vectors; the same is true for the product

$$g^{jk} n_k \frac{\partial}{\partial x^j} = n^j \frac{\partial}{\partial x^j} = \mathbf{n} \cdot \nabla \tag{7b}$$

in the diffusion term.

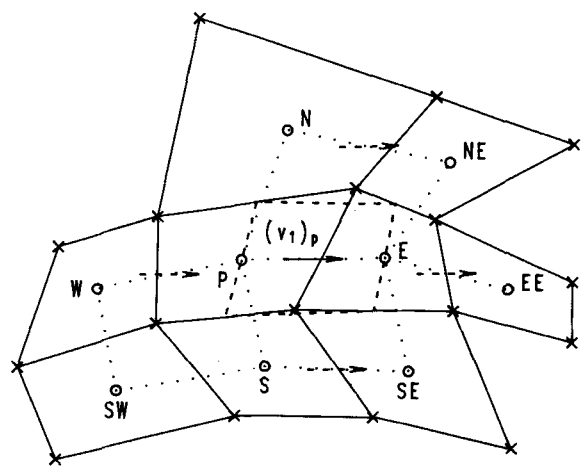

Figure 1. The grid (see Appendix). The dashed arrows show the velocity vectors projected on $\overrightarrow{PE}$, which are neighbours of $(v_1)_P$ (i.e. $(v'_1)_E$, $(v'_1)_W$, $(v'_1)_N$ and $(v'_1)_S$)

Equation (6) can now be discretized using the control volume formulation described in Reference 15. For the v_1-equation the discretized equation may be written

$$a_p(v_1)_p = \sum a_{nb}(v_1')_{nb} + b, \tag{8}$$

where b is the source containing the pressure gradient and the part of the diffusion terms which contains the cross derivative. The prime denotes velocity parallel to the $(v_1)_p$-velocity and is calculated as

$$(v_1')_{nb} = \mathbf{v}_{nb} \cdot (\mathbf{g}_1)_p = (v^j \mathbf{g}_j)_{nb} \cdot (\mathbf{g}_1)_p = (g^{kj} v_k \mathbf{g}_j) \cdot (\mathbf{g}_1)_p. \tag{9}$$

The v_2- and v_3-equations are discretized in the same way. The a_e-coefficient in equation (8), for instance, contains convective contributions such as $(\mathbf{v} \cdot \mathbf{A})_e$ and diffusive contributions such as $\nu(\mathbf{A} \cdot \nabla)_e$ (see equations (7)), where $\mathbf{A}_e$ denotes the vector area of the east face of the control volume.

A discretized equation similar to equation (8) was used by Malin *et al.*[4] and Karki.[5] The derivation leading to equation (8) was, however, not shown by these authors.

To make it possible to solve the velocities using the usual TDM algorithm, equation (8) is rewritten so that (as was done in Reference 5)

$$a_p(v_1)_p = \sum a_{nb}(v_1)_{nb} + b + b_{curv}, \tag{10}$$

where the source term b_{curv} now contains

$$b_{curv} = \sum a_{nb}[(v_1')_{nb} - (v_1)_{nb}].$$

The equations are solved using the SIMPLEC algorithm[16] or the PISO algorithm.[17] The four main features are: staggered grids for the velocities; formulation of the difference equations in implicit, conservative form using hybrid upwind/central differencing; rewriting of the continuity equation as an equation (two equations in the case of PISO) for the pressure correction; and iterative solving of the equations using TDMA.

3. ADVANTAGES OF THE FORMULATION

In most studies of deriving discretized equations for flow in complex geometries, the terms due to curvature/divergence and non-orthogonality of the grid have been included using Christoffel symbols and metric tensors. Since the number of these terms is rather large, it is very cumbersome and may also be inaccurate (there appear terms containing up to the third derivative of the grid co-ordinates). This is not the case with the present formulation.

It is well known that upwind differencing gives rise to numerical diffusion. For polar co-ordinates, or curved grids in general, another type of error occurs and becomes particularly serious when the flow is not aligned with the grid lines. Even if the *magnitude* of the velocity component is well approximated by estimating the face value of v_1 (for example) with its node value, the *direction* of v_1 is not. This was recognized by Galphin *et al.*,[18] who suggested the introduction of a correction velocity, weighted with a factor ω $(0 < \omega < 1)$ depending on the curvature of the flow relative to the grid (cylindrical polar grid). The value of ω is zero if the flow is aligned with the grid.

In the present work this problem is, in our opinion, solved in a more general and straightforward way. The velocity vectors $\mathbf{v}_{nb}$ (nb = neighbour) are projected in the direction of the velocity component at the control volume p. This means that all the neighbours v_{1nb}' (prime denotes projected velocity) of v_{1p} have the same direction. In this way a solution is found to the problem of

estimating a face value of v_1 having an incorrect direction. The same is true of the v_2- and v_3-equations.

4. EXAMPLES OF TEST PROBLEMS

A number of test cases have been calculated where the exact solutions are known, such as rotating Couette flow, Jeffery–Hamel flow and other cases where measurements are available for comparison, and the code was shown to produce accurate results.[19,20] Two examples are shown here.

4.1. Uniform flow using a cylindrical mesh

This test case, which is taken from Galphin *et al.*,[18] has been chosen in order to estimate how much better results can be obtained if the curvature effects are included by projecting the velocities rather than using curvature source terms.

The configuration with the grid is shown in Figure 2. Since we want to estimate the errors for upwind differencing, the viscosity is set to zero. The density is constant and the boundary conditions are

$$v_2 \equiv v_r = U \cos \alpha, \qquad v_1 \equiv v_\phi = -U \sin \alpha,$$

which also, together with $p = 0$, is the exact solution.

The flow has been calculated with the standard treatment of curvature terms and with the procedure of projecting the velocities. The maximal error in the calculated velocities is 8·5% and 0·5% of U for the two cases respectively. In Figure 3 the contours of the pressure are presented.

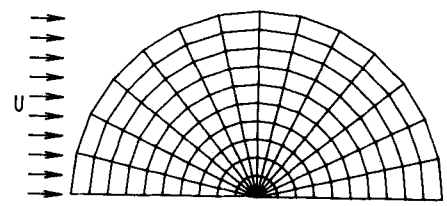

Figure 2. Configuration with grid

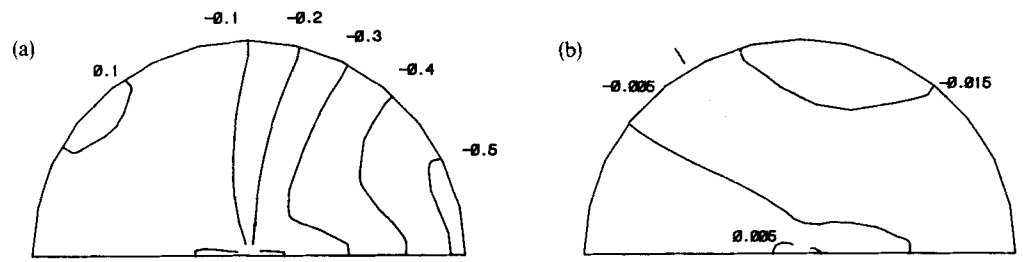

Figure 3. Contours of isobars. Numbers denote pressure scaled with dynamic pressure, $\rho U^2/2$. (a) Non-projected velocities. (b) Projected velocities

4.2. Flow inside a channel with a smooth expansion

Napolitano and Orlandi[21] reported on the outcome of a workshop of the International Association for Hydraulic Research Working Group on Refined Modelling of Flows. Fifteen participating groups returned results on a test case dealing with flow in a plane channel; see Figure 4(a). The lower boundary (solid wall) of the channel is given by

$$y_1 = [\tanh(2-30x/Re)-\tanh(2)]/2$$

for $0 \leqslant x \leqslant x_{out} = Re/3$. The upper boundary (symmetry plane) is located at $y_u = 1$.

The inlet boundary conditions are given in terms of the Cartesian velocity components u and v as

$$\left.\begin{aligned} u &= 3(y - y^2/2) \\ v &= 0 \end{aligned}\right\} \quad \text{for } x = 0,\ 0 \leq y \leq 1.$$

At the wall the no-slip condition is used, and symmetry is enforced at $0 \leq x \leq x_{out}$, $y = y_u$. We specified the outlet boundary conditions as zero gradient in the x-direction for v_1 and v_2. A mesh

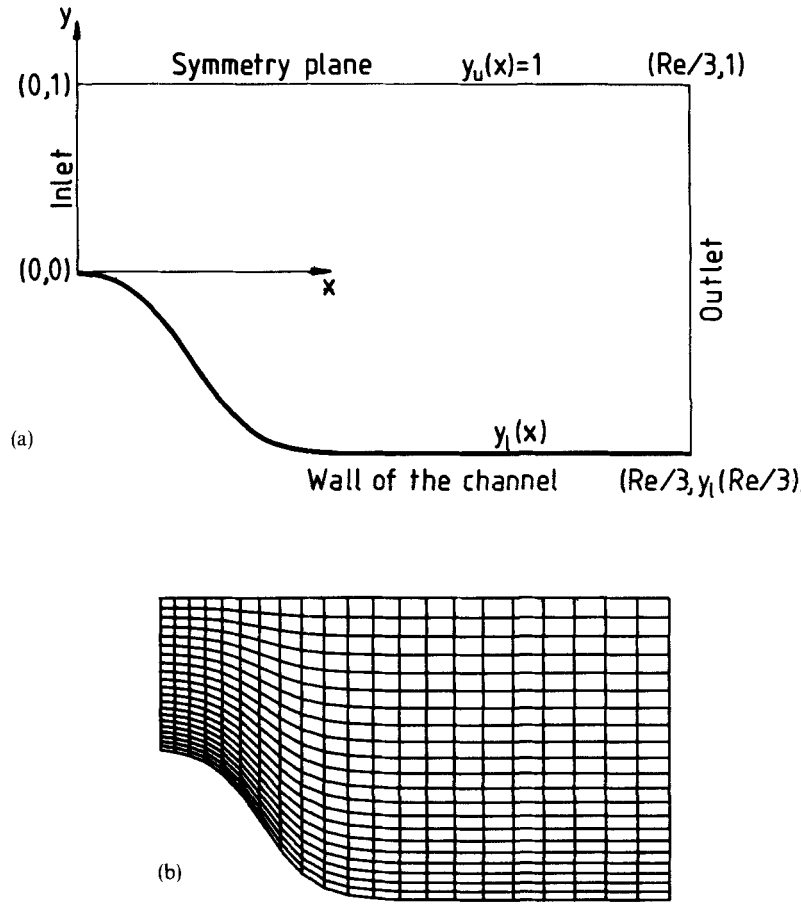

Figure 4. (a) Configuration. (b) Grid.

of 21 × 21 grid points was used. Figure 4(b) shows our particular grid. Two flows were selected as test cases at the workshop, $Re = 10$ and $Re = 100$. The former was chosen because of its rather distorted geometry and the latter to assess the dependence of the convergence rate on Re. We have studied the flow at $Re = 10$. The results are also presented as pressure and vorticity distributions along the wall; see Figures 5 and 6. The reference curve is taken from a finite element calculation where the solution was made grid-independent. The pressure has a singular point at the inlet. This is because fully developed Poiseuille flow conditions have been prescribed at the inlet, in spite of the non-zero slope of the wall at $x = 0$.

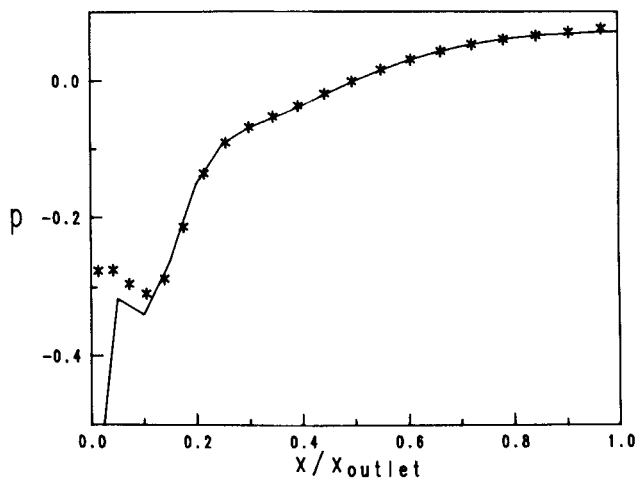

Figure 5. Pressure distributions at the wall: *, present calculation; solid line, reference calculation[21]

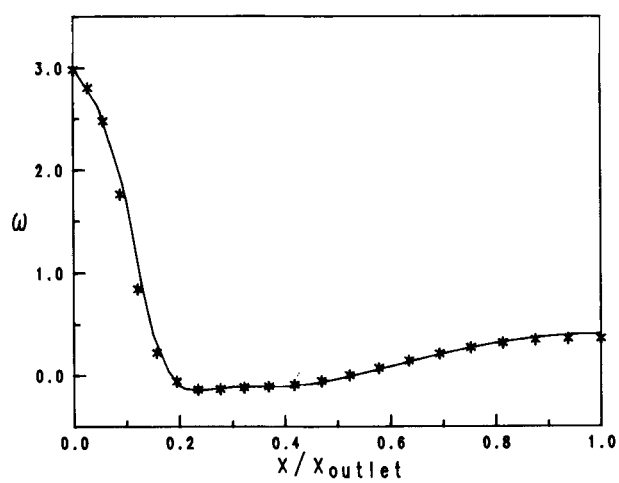

Figure 6. Vorticity distributions at the wall: *, present calculation; solid line, reference calculation[21]

5. CONCLUSIONS

This paper has presented the mathematical derivation of a novel formulation where a local co-ordinate system is set up at each point P. This means that most of the terms vanish due to curvature and/or divergence/convergence of the grid lines, so that the momentum equations can be formulated in a simpler way and probably also more accurately.

It has been shown that when using upwind differencing the present formulation is more accurate than the conventional formulation when the flow is not aligned with the grid lines in a curved grid. This is due to the fact that even if the *magnitude* is well approximated, the direction of the velocity component is not. Since in the present formulation the *direction* of the velocity components does not change, this problem does not arise.

A code has been developed and was applied here to two laminar test cases. No stability problems or convergence problems have been encountered. Relaxations of typically 0·5 on the momentum equations have been used.

The standard k–ε turbulence model has recently been implemented in the code and some calculations have been performed.[20] More details on the code are available in Reference 19. In the near future we plan to extend the code to cover three-dimensional geometries as well.

APPENDIX

Integration of a vector field

Let B be a tensor of second rank of mixed variance. This can be integrated over a volume V using the Gauss theorem:[14]

$$\int_V B^j_{i,j}\mathbf{g}^i \mathrm{d}V = \int_S B^j_i n_j \mathbf{g}^i \mathrm{d}S.$$

The curvature effects are now (on the RHS of the equation) accounted for through the variation of the contravariant base vectors over the area S; if they are constant, these effects will vanish.

It may be noted that if the contravariant base vectors do not change, then this is valid for the covariant base vectors as well, owing to the relation[12]

$$\mathbf{g}^i \cdot \mathbf{g}_j = \delta^i_j.$$

The grid

A grid is shown in Figure 1. The crosses define the corners of the scalar control volumes and the circles define the scalar nodes. The position of a scalar node is defined as the average of its four cell corners. The lines which connect these nodes (dotted lines in Figure 1) define the direction of the base vectors (see below).

The v_1-control volume is staggered in the positive x^1-direction; it is outlined with dashed lines in Figure 1. Its east face, for example, is defined as being midway between the east faces of scalar control volumes P and E.

Change of base vectors

$\overrightarrow{\mathrm{PE}}(=(\mathbf{g}_1)_\mathrm{P})$, $\overrightarrow{\mathrm{WP}}$, $\overrightarrow{\mathrm{E(EE)}}$, $\overrightarrow{\mathrm{N(NE)}}$, $\overrightarrow{\mathrm{S(SE)}}$, etc. (see Figure 1) define the directions of the covariant unit base vectors $\mathbf{g}_i$. The dashed arrows show the $(\mathbf{g}_1)_\mathrm{nb}$-vectors changed so that they are parallel (or rather, equal) to the $(\mathbf{g}_1)_\mathrm{P}$-vector; the dashed arrows can also be said to be the $(\mathbf{g}_1)_\mathrm{P}$-vector moved to the positions of the $(\mathbf{g}_1)_\mathrm{nb}$-vectors.

When the $(\mathbf{g}_1)_{nb}$-vectors are assumed to be equal to $(\mathbf{g}_1)_P$, they must, apart from being parallel, also be of equal *length*. All base vectors are, however, of equal length, since the x^i-co-ordinates are chosen in physical units.

Formulae for the metric tensor g^{ij}

Since the grid is locally rectilinear, the formula for the metric tensor g^{ij} for the v_1-velocity control volume in Figure 1 is[13]

$$g^{11} = 1/g, \qquad g^{12} = -(\cos\alpha)/g, \qquad g^{21} = g^{12}, \qquad g^{22} = 1/g,$$

where α denotes the angle between $\overrightarrow{PE}$ and $\overrightarrow{PN}$, and g is the determinant of the covariant metric tensor g_{ij} and has the form

$$g = 1 - \cos^2\alpha.$$

ACKNOWLEDGEMENTS

We wish to express our thanks to our supervisor Prof. Erik Olsson who has been very encouraging during this study. We are also indebted to Prof. Olle Brander at the Department of Theoretical Physics and Mechanics, Chalmers University of Technology, who gave valuable comments on the derivation in Section 2.

This work was financed by the Swedish Council for Building Research, the Swedish Board for Technical Development and many Swedish companies with an interest in turbomachinery technology.

The names of the authors appear in alphabetical order.

REFERENCES

1. S. B. Pope, 'The calculation of turbulent recirculating flows in general coordinates', *J. Comput. Phys.* **26,** 197–217 (1978).
2. G. Berge, 'Numerisk programsystem basert på fleirdimensjonale ortogonale koordinater for simulering av forbrenning, masse og varmetransport' (in Norwegian), Institutt for teknisk varmelaere, Norges Tekniska Högskole, Trondheim, 1982.
3. G. D. Raithby, P. F. Galphin and J. P. Van Doormaal, 'Prediction of heat and fluid flow in complex geometries using general coordinates', *Numer. Heat Transfer*, **9,** 125–142 (1986).
4. M. R. Malin, H. I. Rosten, D. G. Tatchell and D. B. Spalding, 'Application of PHOENICS to flow around ships' hulls', *Second Int. Symp. on Ship Viscous Resistance*, Gothenburg, 1985.
5. K. C. Karki, 'A calculation procedure for viscous flows at all speeds in complex geometries', *Ph.D. Thesis*, University of Minnesota, 1986.
6. S. Parameswaran, 'Finite volume equations for fluid flow based on non-orthogonal velocity projections', *Ph.D. Thesis*, University of London, 1986.
7. I. Demirdzic, A. D. Gosman and R. I. Issa, 'A finite-volume method for the prediction of turbulent flow in arbitrary geometries', *Proc. 7th Int. Conf. on Numerical Methods in Fluid Dynamics*, Springer Verlag, 1980.
8. A. Nakayama, 'A numerical method for solving momentum equations in generalized coordinates (its application to three-dimensional separated flows)', *J. Fluids Eng.*, **107,** 49–54 (1985).
9. C. Hah and B. Lakshiminarayana, 'The computation of a highly curved mixing layer with an algebraic Reynolds-stress closure scheme', in S. J. Kline *et al.* (eds), *Proc. 1980–81 AFOSR–HTTM–Stanford Conf. on Complex Turbulent Flows: Comparison of Computation and Experiment. Vol. 3*, 1982.
10. I. Demirdzic, A. D. Gosman and R. I. Issa, 'Some separated flow cases', in S. J. Kline *et al.* (eds), *1980–81 AFOSR–HTTM–Stanford Conf. on Complex Turbulent Flows: Comparison of Computation and Experiment. Vol. 3*, 1982.
11. R. Aris, *Vectors, Tensors and the Basic Equations of Fluid Mechanics*, Prentice-Hall Inc., Englewood Cliffs, NJ, 1962.
12. B. Spain, *Tensor Calculus*, 3rd Edn, University Mathematical Texts, Oliver and Boyd, Edinburgh, 1960.
13. W. Flugge, *Tensor Analysis and Continuum Mechanics*, Springer-Verlag, Berlin, 1972.
14. F. Irgens, *Tensoranalyse og kontinuumsmekanikk* (in Norwegian), del III, Institutt for mekanikk, Norges Tekniska Högskole, Trondheim, 1966.
15. S. V. Patankar, *Numerical Heat Transfer and Fluid Flow*, McGraw-Hill, Washington, 1980.

16. J. P. Van Doormaal and G. D. Raithby, 'Enhancements of SIMPLE method for predicting incompressible fluid flows', *Numer. Heat Transfer*, **7**, 147–163 (1984).
17. R. I. Issa, 'Solution of the implicitly discretised fluid flow equations by operator-splitting', *J. Comput. Phys.*, **62**, 40–65 (1986).
18. P. F. Galphin, G. D. Raithby and J. P. Van Doormaal, 'Discussion of upstream-weighted advection approximations for curved grids', *Numer. Heat Transfer*, **9**, 241–246 (1986).
19. L. Davidson and P. Hedberg, 'FLUX2D: a finite-volume computer program written in general non-orthogonal coordinates for calculation of two-dimensional turbulent flow', *Report 88/1*, Department of Applied Thermodynamics and Fluid Mechanics, Chalmers University of Technology, Göteborg, 1988.
20. L. Davidson, P. Hedberg and E. Olsson, 'A finite-volume computer program for turbulent flow in complex geometries', accepted for presentation at the *7th Int. Conf. on Finite Element Methods in Fluid Problems*. Huntsville, Alabama, April 1989.
21. M. Napolitano and P. Orlando, 'Laminar flow in complex geometry: a comparison', *Int. j. numer. methods fluids*, **5**, 667–683 (1985).